Acta Mech 228, 3771–3787 (2017)
DOI 10.1007/s00707-017-1903-7

ORIGINAL PAPER

Alba Sofi

Euler–Bernoulli interval finite element with spatially varying uncertain properties

Received: 15 January 2017 / Revised: 14 April 2017 / Published online: 8 July 2017

Abstract The formulation of an Euler–Bernoulli beam finite element with spatially varying uncertain properties is presented. Uncertainty is handled within a non-probabilistic framework resorting to a recently proposed *interval field* model able to quantify the dependency between adjacent values of an interval quantity that cannot differ as much as values that are further apart. Once the interval element stiffness matrix is defined, the set of linear interval equations governing the interval global displacements of the finite element model is derived by performing a standard assembly procedure. Then, the bounds of the interval displacements and bending moments are determined in approximate explicit form by applying a *response surface approach* in conjunction with the so-called *improved interval analysis via extra unitary interval*. For validation purposes, numerical results concerning both statically determinate and indeterminate beams with interval Young's modulus are presented.

1 Introduction

The growing awareness of the influence of inevitable uncertainties on the performance of engineering systems has stimulated an increasing interest toward the development of efficient non-deterministic numerical procedures to achieve more robust and reliable designs (see, e.g., [1,2]). In this context, a major challenge is to incorporate the non-deterministic input parameters into standard finite element (FE) models and then develop efficient propagation strategies. This task is commendably accomplished within the probabilistic framework by the well-established stochastic finite element method (SFEM) (see, e.g., [3]) which may be regarded as the most powerful tool currently available to integrate random input parameters into numerical modeling. Recently, much research effort has been devoted to develop a similar tool within a non-probabilistic framework, giving rise among others to the so-called interval finite element method (IFEM) where the uncertain parameters are modeled as interval variables with given lower bound (LB) and upper bound (UB) [4]. Such a model proves to be very useful when available data are insufficient to build a credible probabilistic distribution of the uncertain parameters, as it happens in early design stages [5]. Furthermore, the propagation of interval uncertainty usually requires less intensive calculations. The main drawback of the interval model is the overestimation of the interval solution range due to the so-called *dependency phenomenon* [4] which often leads to useless results in the context of engineering design. Several versions of the IFEM have been proposed with the purpose of finding sharp bounds of the interval output [6–11]. For a general overview of the state-of-the-art and recent

A. Sofi
Department of Architecture and Territory (dArTe), Inter-University Centre of Theoretical and Experimental Dynamics, University "Mediterranea" of Reggio Calabria, 89124 Reggio Calabria, Italy

A. Sofi (✉)
Department of Engineering Science, University of Oxford, Parks Road, Oxford OX1 3PJ, UK
E-mail: alba.sofi@unirc.it

advances in interval finite element analysis, readers are referred to [12,13]. An effective remedy to the drastic overestimation affecting interval-based structural analyses is the *improved interval analysis* [14] which overcomes the main drawbacks of the *classical interval analysis* (*CIA*) by using a particular unitary interval, called *extra unitary interval* (*EUI*).

Besides the limitation of the effects of the *dependency phenomenon*, other two challenging tasks need to be tackled in the development of IFEMs: to properly take into account the spatial character of uncertainties, like material or geometric properties to build computationally efficient propagation procedures.

In standard IFEMs, spatially variable interval uncertainties, such as Young's modulus of the material or plate thickness, are commonly discretized assigning an interval-valued parameter to each FE. The uncertain property is thus represented over the whole domain by a set of interval variables which are by definition unable to account for mutual dependency. Indeed, this approach relies on the extreme assumption of spatial independency of uncertainties which is both unrealistic and computationally expensive due to the large number of interval variables involved. Alternatively, a single interval variable over the entire model can be assumed which implies the introduction of the opposite extreme hypothesis of total spatial dependency.

In order to provide a more realistic description of spatially varying interval uncertainties, the *interval field* model [15,16] has been recently introduced as the natural extension of the random field concept [17] to the non-probabilistic framework. The key idea behind the interval field model is to express the uncertain property as superposition of deterministic basis functions representing the spatial character, weighted by independent interval coefficients representing the uncertainty. Different definitions of the interval field have been introduced in the literature, such as those based on the Inverse Distance Weighting interpolation (IDW) or the Local Interval Field Decomposition method (LIFD) [18,19]. Recently, the author contributed to the development of an interval field model based on the *IIA via EUI* [20]. Such a model accounts for the dependency between interval values of an uncertain property at various locations by introducing a deterministic, symmetric, non-negative, bounded function, called *spatial dependency function*, playing the same role of the autocorrelation function in random field theory. The static analysis of both Euler–Bernoulli [21] and Timoshenko [22] beams with uncertain properties represented by means of the interval field model based on the *IIA via EUI* has been performed by applying the so-called *Interval Rational Series Expansion* (*IRSE*) in the context of a finite difference scheme. Recently, Wu and Gao [23] proposed a computational scheme, called *extended unified interval stochastic sampling*, to perform a hybrid uncertain static analysis of structures involving random and interval fields.

The interval field model based on the *IIA via EUI* [20] exhibits some important advantages with respect to the above mentioned models, i.e.: (i) the basis functions can be readily defined based on the knowledge of the eigenvalues and eigenfunctions of the *spatial dependency function*, which should reproduce as closely as possible the real spatial variability of the uncertain property; (ii) the interval coefficients are represented by the *EUI*s which do not follow the rules of the *CIA* and thus allow one to limit the overestimation of the solution range due to the *dependency phenomenon*; (iii) the dimensionality of uncertainty is drastically reduced since it does not depend on the number of FEs of the mesh.

The aim of the present paper is to incorporate the interval field representation of uncertain input properties into the standard finite element procedure. Without loss of generality, attention is focused on the formulation of an Euler–Bernoulli beam element with uncertain Young's modulus described as an interval field based on the *IIA via EUI*. By applying the standard energy approach, the interval element stiffness matrix is derived as sum of the nominal value plus an interval deviation. The latter is given by the superposition of independent contributions which are identified by the associated *EUI*s. Such a feature enables to apply a standard assembly procedure to derive the set of linear interval equations governing the interval global displacements of the FE model. Then, an efficient procedure for evaluating the bounds of the interval response is developed by applying a *response surface approach* [24] in conjunction with the *IIA via EUI*. The proposed solution strategy allows a drastic reduction of the computational effort compared to combinatorial procedures. Another remarkable feature of the presented method is the capability of providing very accurate estimates of secondary variables as well.

The selected case studies concern both statically determinate and indeterminate beams, say a cantilever beam and a fixed-simply supported beam with interval Young's modulus under deterministic static loads. The influence of the spatial dependency of the uncertain property is investigated by appropriate comparisons with the results provided by the standard IFEM under the assumption of independent interval Young's moduli for each FE. Furthermore, the accuracy and efficiency of the presented IFE formulation are demonstrated by contrasting the proposed bounds of the response with those provided by a burdensome combinatorial procedure, known as *vertex method* (VM) [25].

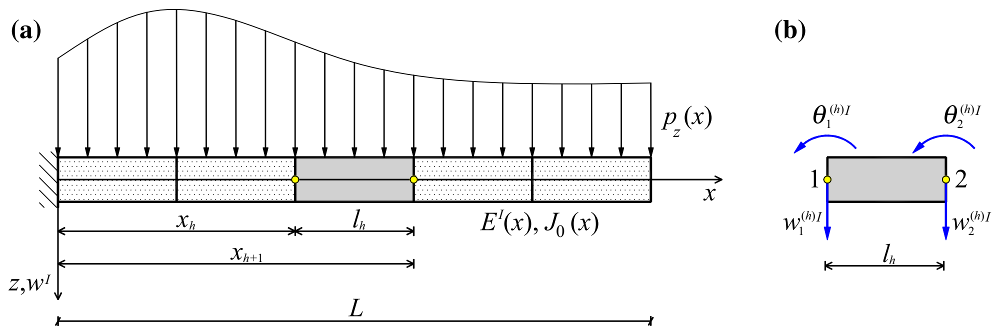

Fig. 1 **a** Euler–Bernoulli beam under distributed load with uncertain Young's modulus; **b** interval Euler–Bernoulli beam FE

The paper is organized as follows: in Sect. 2, the main features of the interval field model based on the *IIA via EUI* are briefly summarized; Sect. 3 is devoted to the formulation of the Euler–Bernoulli beam element with interval Young's modulus field; Sects. 4 and 5 focus on the development of an efficient procedure for the evaluation of the bounds of the interval displacements and bending moments; finally, in Sect. 6, numerical results are presented.

2 Euler–Bernoulli beam with spatially varying interval Young's modulus

Let us consider a linear elastic Euler–Bernoulli beam of length L subjected to a deterministic transversally distributed load $p_z(x)$ (see Fig. 1). The geometric properties of the beam are assumed to be known deterministically, while Young's modulus of the material is treated as an uncertain parameter in the context of the interval model of uncertainty [4]. Specifically, in order to take into account the inherent spatial variability, the uncertain material property is represented as an interval field, $E^I(x)$, adopting a recently proposed model [20–22] based on the so-called *improved interval analysis via extra unitary interval* (*IIA via EUI*) [14]. For the sake of clarity, first the main features of the assumed interval field model are briefly outlined, and then the equations governing the response of the beam with interval Young's modulus are formulated.

Let the uncertain Young's modulus be described by the following interval function:

$$E^I(x) = \left[\underline{E}(x), \bar{E}(x)\right] = E_0\left[1 + B^I(x)\right], \quad x \in [0, L] \tag{1}$$

where the superscript I denotes interval quantities; $\underline{E}(x)$ and $\bar{E}(x)$ are the lower bound (LB) and upper bound (UB). The midpoint value $E_0 \in \mathbb{R}$, taken constant over the whole domain $[0, L]$, and the deviation amplitude $\Delta E(x)$ of the interval function $E^I(x)$ are given, respectively, by:

$$\text{mid}\left\{E^I(x)\right\} = \frac{\bar{E}(x) + \underline{E}(x)}{2} \equiv E_0, \tag{2.1}$$

$$\Delta E(x) = \frac{\bar{E}(x) - \underline{E}(x)}{2} \equiv E_0 \Delta B(x), \quad x \in [0, L] \tag{2.2}$$

where mid{•} denotes the midpoint of the interval quantity into curly parentheses. In Eq. (1), $B^I(x) = \left[\underline{B}(x), \bar{B}(x)\right]$ denotes a dimensionless interval function having zero midpoint and deviation amplitude $\Delta B(x) < 1$, so that the midpoint value of $E^I(x)$ coincides with the nominal value of the uncertain material property (see Eq. (2.1)).

The spatial dependency of the interval field is assumed to be governed by a real, deterministic, symmetric, non-negative function, $\Gamma_B(x, \xi)$, defined as follows:

$$\Gamma_B(x, \xi) = \text{mid}\left\{B^I(x)B^I(\xi)\right\} \equiv \frac{\text{mid}\left\{E^I(x)E^I(\xi)\right\}}{(E_0)^2} - 1, \quad x, \xi \in [0, L]. \tag{3}$$

Notice that $\Gamma_B(x, \xi)$, named *spatial dependency function*, represents the midpoint of the dimensionless interval function $B^I(x)B^I(\xi)$.

By viewing the function $\Gamma_B(x, \xi)$ as the non-probabilistic counterpart of the autocorrelation function characterizing probabilistically a random field, the following Karhunen–Loève (KL)-like decomposition can be applied [26]:

$$\Gamma_B(x,\xi)=\sum_{i=1}^{\infty}\lambda_i\psi_i(x)\psi_i(\xi)\Rightarrow\Gamma_B(x,x)\equiv\text{mid}\left\{\left(B^I(x)\right)^2\right\}=\sum_{i=1}^{\infty}\lambda_i\psi_i^2(x)\tag{4}$$

where λ_i, $(i=1,2,\ldots)$, is the ith *eigenvalue* of the bounded, symmetric, non-negative function, $\Gamma_B(x,\xi)$, and $\psi_i(x)$, $(i=1,2,\ldots)$, is the corresponding *eigenfunction*, solutions of the following homogeneous Fredholm integral equation of the second kind:

$$\int_0^L\Gamma_B(x,\xi)\psi_i(x)\mathrm{d}x=\lambda_i\psi_i(\xi).\tag{5}$$

The eigenvalues, λ_i, are real positive numbers, and the associated eigenfunctions, $\psi_i(x)$, are real functions satisfying the following orthogonality condition:

$$\int_0^L\psi_i(x)\psi_j(x)\mathrm{d}x=\begin{cases}1 & \text{if} \quad i=j\\ 0 & \text{if} \quad i\neq j.\end{cases}\tag{6}$$

By exploiting the properties of the so-called *EUI* [14], $\hat{e}_i^I=[-1,+1]$, the definition (3) of the function $\Gamma_B(x,\xi)$ and the decomposition (4) truncated to the first M terms lead to the following expression of the dimensionless interval function $B^I(x)$:

$$B^I(x)=\sum_{i=1}^{M}\sqrt{\lambda_i}\;\psi_i(x)\hat{e}_i^I,\quad x\in[0,L].\tag{7}$$

Then, replacing Eq. (7) into Eq. (1), the interval field $E^I(x)$ can be recast as:

$$E^I(x)=E_0\left[1+\sum_{i=1}^{M}\sqrt{\lambda_i}\;\psi_i(x)\hat{e}_i^I\right],\quad x\in[0,L]\tag{8}$$

with the LB and UB given by the following relationships:

$$\underline{E}(x)=E_0\left[1-\Delta B(x)\right];\quad \bar{E}(x)=E_0\left[1+\Delta B(x)\right],\quad x\in[0,L]\tag{9.1,2}$$

where

$$\Delta B(x)=\frac{\Delta E(x)}{E_0}=\sum_{i=1}^{M}\left|\sqrt{\lambda_i}\;\psi_i(x)\right|,\quad x\in[0,L]\tag{10}$$

with $|\bullet|$ denoting the absolute value of $\bullet$.

It is worth remarking that the interval field model based on the *IIA via EUI* (8) describes separately the spatial dependency and the uncertainty of Young's modulus by means of the deterministic functions $\sqrt{\lambda_i}\;\psi_i(x)$ and the associated *EUI*s, respectively. This is a highly desirable feature in the framework of interval field representation (see, e.g., [19]) which enables to apply propagation techniques commonly used for discrete input interval variables. In this regard, it is also observed that the interval field model based on the *IIA via EUI* ensures substantial computational savings since the number of independent interval parameters is no more related to the number of FEs in the mesh, but it is always given by the truncation order of the KL-like decomposition, say M.

In analogy with the autocorrelation function characterizing a random field, the analytical expression of the *spatial dependency function*, $\Gamma_B(x,\xi)$, needs to be postulated in a physically consistent way. Without loss of generality, the following exponential form is assumed:

$$\Gamma_B(x,\xi)=C_B^2\exp\left(-\frac{|x-\xi|}{l_B}\right)\tag{11}$$

where the parameters C_B and l_B may be regarded, respectively, as the non-probabilistic counterpart of the standard deviation and correlation length in random field theory. Indeed, C_B is a parameter affecting the deviation amplitude of the interval field and thus the degree of uncertainty, while l_B rules the spatial dependency of the uncertain property. If $l_B \rightarrow \infty$, the *spatial dependency function* in Eq. (11) approaches the value C_B^2 and the dimensionless interval function $B^I(x)$ reduces to a symmetric interval variable, i.e., $B^I(x) \equiv b^I = b\hat{e}^I$ with deviation amplitude $b = C_B$. At the opposite extreme, as $l_B \rightarrow 0$, the uncertain Young's modulus becomes spatially independent [20]. The eigenvalues and eigenfunctions of the exponential function in Eq. (11) can be evaluated in analytical form [26]. It is worth mentioning that different definitions of the *spatial dependency function*, such as the squared exponential, can be assumed as well.

The transverse displacement of the beam with interval Young's modulus (8) is described by an interval field $w^I(x)$ ruled by the following fourth-order ordinary interval differential equation:

$$\frac{\mathrm{d}^2}{\mathrm{d}x^2}\left[E^I(x)J_0(x)\frac{\mathrm{d}^2 w^I(x)}{\mathrm{d}x^2}\right] = p_z(x) \tag{12}$$

supplemented by the pertinent kinematic and static boundary conditions, herein assumed deterministic, i.e., independent of interval variables. In the previous equation, $J_0(x)$ denotes the moment of inertia of the beam cross section. Upon replacing Eq. (8) for $E^I(x)$, Eq. (12) reads:

$$E_0\frac{\mathrm{d}^2}{\mathrm{d}x^2}\left[J_0(x)\frac{\mathrm{d}^2 w^I(x)}{\mathrm{d}x^2}\right] + E_0\sum_{i=1}^{M}\sqrt{\lambda_i}\,\hat{e}_i^I\frac{\mathrm{d}^2}{\mathrm{d}x^2}\left[\psi_i(x)J_0(x)\frac{\mathrm{d}^2 w^I(x)}{\mathrm{d}x^2}\right] = p_z(x). \tag{13}$$

Notice that, dropping the second term on the left-hand side, Eq. (13) yields the equilibrium equation of the beam with nominal value of the modulus of elasticity, E_0.

By applying interval extension [4], the interval total potential energy (ITPE) of the beam takes the following form:

$$\Pi[w^I(x)] = \Phi^I - W^I = \frac{1}{2}\int_0^L E^I(x)J_0(x)\left(\chi^I(x)\right)^2\mathrm{d}x - \int_0^L p_z(x)w^I(x)\mathrm{d}x \tag{14}$$

where Φ^I and W^I denote the interval strain energy stored in the beam and the interval work done by the external loads, respectively; $E^I(x)$ is the interval Young's modulus given by Eq. (8), and $\chi^I(x)$ is the interval flexural curvature, given by:

$$\chi^I(x) = -\frac{\partial^2 w^I(x)}{\partial x^2}. \tag{15}$$

In Ref. [21], an approximate solution of Eq. (13) is pursued by applying the so-called *Interval Rational Series Expansion* (*IRSE*) in the context of a finite difference scheme. The aim of the present study is to develop an interval finite element approach based on the formulation of an interval Euler–Bernoulli FE incorporating the interval field model of the uncertain Young's modulus based on the *IIA via EUI*.

3 Formulation of the interval Euler–Bernoulli beam finite element

Let us discretize the beam with interval Young's modulus into N two-node beam FEs of length $l_h = L/N$ (see Fig. 1a). According to the standard formulation of the Euler–Bernoulli beam FE, the interval transversal displacement field within the hth FE (see Fig. 1b) is expressed as follows:

$$w^{(h)I}(x) = \mathbf{N}^{(h)}(x)\mathbf{d}^{(h)I} \tag{16}$$

where $\mathbf{N}^{(h)}(x)$ is the (1×4) matrix collecting the cubic Hermite interpolation functions $\phi_j^{(h)}(x)$, $j = 1, 2, \ldots, 4$, which are the same as those used within a deterministic context; $\mathbf{d}^{(h)I}$ is the interval vector listing the nodal generalized displacements (see Fig. 1b):

$$\mathbf{d}^{(h)I} = \left[\, w_1^{(h)I}\ \theta_1^{(h)I}\ w_2^{(h)I}\ \theta_2^{(h)I}\,\right]^{\mathrm{T}} \tag{17}$$

where

$$w_1^{(h)I} = w^{(h)I}(x_h); \quad \theta_1^{(h)I} = -\left.\frac{\partial w^{(h)I}(x)}{\partial x}\right|_{x=x_h}; \tag{18.1,2}$$

$$w_2^{(h)I} = w^{(h)I}(x_{h+1}); \quad \theta_2^{(h)I} = -\left.\frac{\partial w^{(h)I}(x)}{\partial x}\right|_{x=x_{h+1}}. \tag{18.3,4}$$

The interval curvature $\chi^{(h)I}(x)$ can be expressed in terms of nodal displacements as:

$$\chi^{(h)I}(x) = -\frac{\partial^2 w^{(h)I}(x)}{\partial x^2} = \mathbf{B}^{(h)}(x)\mathbf{d}^{(h)I} \tag{19}$$

where $\mathbf{B}^{(h)}(x) = -\partial^2\mathbf{N}^{(h)}(x)/\partial x^2$ is the (1×4) curvature-displacement matrix.

Following the standard energy formulation, the interval Euler–Bernoulli beam FE can be formulated by evaluating the ITPE of the beam (14) as sum of the contributions, $\Pi^{(h)}[\mathbf{d}^{(h)I}]$, associated to the N FEs. Specifically, substituting Eqs. (16) and (19) into Eq. (14), the discretized form of the ITPE functional yields the following quadratic form in the interval nodal displacements:

$$\begin{aligned}\Pi[\mathbf{d}^{(h)I}] &= \sum_{h=1}^{N}\Pi^{(h)I} = \sum_{h=1}^{N}\left(\Phi^{(h)I} - W^{(h)I}\right)\\ &= \frac{1}{2}\sum_{h=1}^{N}\mathbf{d}^{(h)I^{\mathrm{T}}}\left(\int_{x_h}^{x_{h+1}} E^I(x)J_0(x)\mathbf{B}^{(h)^{\mathrm{T}}}(x)\mathbf{B}^{(h)}(x)\mathrm{d}x\right)\mathbf{d}^{(h)I}\\ &\quad -\sum_{h=1}^{N}\mathbf{d}^{(h)I^{\mathrm{T}}}\left(\int_{x_h}^{x_{h+1}}\mathbf{N}^{(h)^{\mathrm{T}}}(x)p_z(x)\mathrm{d}x\right).\end{aligned} \tag{20}$$

Equation (20) can be recast as follows:

$$\Pi[\mathbf{d}^{(h)I}] = \frac{1}{2}\sum_{h=1}^{N}\mathbf{d}^{(h)I^{\mathrm{T}}}\mathbf{k}^{(h)I}\mathbf{d}^{(h)I} - \sum_{h=1}^{N}\mathbf{d}^{(h)I^{\mathrm{T}}}\mathbf{f}^{(h)} \tag{21}$$

where

$$\mathbf{k}^{(h)I} = \int_{x_h}^{x_{h+1}} E^I(x)J_0(x)\mathbf{B}^{(h)^{\mathrm{T}}}(x)\mathbf{B}^{(h)}(x)\mathrm{d}x \tag{22}$$

is the interval element stiffness matrix, and

$$\mathbf{f}^{(h)} = \int_{x_h}^{x_{h+1}}\mathbf{N}^{(h)^{\mathrm{T}}}(x)p_z(x)\mathrm{d}x \tag{23}$$

is the element nodal force vector which is not affected by uncertainty.

Replacing definition (8) of the interval Young's modulus field based on the *IIA via EUI*, the interval element stiffness matrix can be recast as:

$$\mathbf{k}^{(h)I} = \mathbf{k}_0^{(h)} + \sum_{i=1}^{M}\mathbf{k}_i^{(h)}\hat{e}_i^I \tag{24}$$

where

$$\mathbf{k}_0^{(h)} = E_0\int_{x_h}^{x_{h+1}} J_0(x)\mathbf{B}^{(h)^{\mathrm{T}}}(x)\mathbf{B}^{(h)}(x)\mathrm{d}x \tag{25}$$

is the nominal element stiffness matrix, while

$$\mathbf{k}_i^{(h)} = E_0\sqrt{\lambda_i}\int_{x_h}^{x_{h+1}} \psi_i(x)J_0(x)\mathbf{B}^{(h)^{\mathrm{T}}}(x)\mathbf{B}^{(h)}(x)\mathrm{d}x \tag{26}$$

is the deviation matrix associated with the ith term of the KL-like decomposition. The integration in Eq. (26) may be performed either analytically, if the eigenfunctions $\psi_i(x)$ of the *spatial dependency function*, $\Gamma_B(x,\xi)$, and $J_0(x)$ (in the case of non-uniform beams) are known, or numerically. As already mentioned, for the selected exponential form (11) of the function $\Gamma_B(x,\xi)$, the solution of the integral eigenproblem (5) can be derived in closed form, so that analytical expressions of the interval element stiffness matrices can be obtained. To expedite the calculations of integrals (26), a local coordinate may be introduced, as customary in FE procedures.

Then, as in the standard FEM, the interval nodal displacement vector of the hth FE, $\mathbf{d}^{(h)I}$, is related to the global nodal displacements collected into the interval vector $\mathbf{U}^I$ as:

$$\mathbf{d}^{(h)I} = \mathbf{L}^{(h)}\mathbf{U}^I \tag{27}$$

where $\mathbf{L}^{(h)}$ is the connectivity matrix. Then, the assembly procedure yields the following set of linear interval equations governing the equilibrium of the FE model of the beam:

$$\mathbf{K}^I\mathbf{U}^I = \mathbf{F} \tag{28}$$

where

$$\mathbf{K}^I = \mathbf{K}_0 + \sum_{i=1}^{M}\mathbf{K}_i\hat{e}_i^I \tag{29}$$

and

$$\mathbf{F} = \sum_{h=1}^{N}\mathbf{L}^{(h)^{\mathrm{T}}}\mathbf{f}^{(h)} \tag{30}$$

are the interval global stiffness matrix and the nodal force vector, respectively. In Eq. (29), $\mathbf{K}_0$ denotes the nominal global stiffness matrix, defined as

$$\mathbf{K}_0 = \sum_{h=1}^{N}\mathbf{L}^{(h)\mathrm{T}}\mathbf{k}_0^{(h)}\mathbf{L}^{(h)} \tag{31}$$

while $\mathbf{K}_i$ is the global deviation stiffness matrix associated with the ith term of the KL-like decomposition, given by:

$$\mathbf{K}_i = \sum_{h=1}^{N}\mathbf{L}^{(h)\mathrm{T}}\mathbf{k}_i^{(h)}\mathbf{L}^{(h)}. \tag{32}$$

4 Approximate explicit bounds of the interval displacements

The solution set of the interval global equilibrium equations (28), Σ, contains all possible solutions obtained as the *EUI*s, $\hat{e}_i^I = [-1,+1]$, range over their intervals, i.e.:

$$\Sigma = \left\{\mathbf{U}\in\mathbb{R}^n \middle| \mathbf{K}\mathbf{U} = \mathbf{F}, \quad \hat{e}_i \in \hat{e}_i^I = [-1,+1]\right\} \tag{33}$$

where n is the order of the global displacement vector $\mathbf{U}$. The exact evaluation of the solution set is very difficult since, typically, it is described by a complicated region in the output space. In the framework of interval analysis, it is common practice to seek the interval displacement vector $\mathbf{U}^I$, containing the solution set Σ, which has the narrowest interval components. Thus, the aim is the evaluation of the LB and UB of the interval displacement vector $\mathbf{U}^I$, say $\underline{\mathbf{U}}$ and $\bar{\mathbf{U}}$. In this context, the knowledge of the exact or approximate explicit relationship between the interval response and the *EUI*s is highly desirable. In this section, a procedure to derive approximate explicit expressions of the interval displacement components as functions of the *EUI*s is presented.

Let us assume that the jth interval displacement, U_j^I, can be approximated as sum of the nominal value, $U_{0,j}$, plus an interval deviation, i.e.:

$$U_j^I = U_{0,j} + \sum_{i=1}^{M} U_{i,j}^I. \tag{34}$$

The interval deviation is given by the superposition of the contributions, $U_{i,j}^I, i = 1, 2, \ldots, M$, associated with the terms of the KL-like decomposition (8) of the interval Young's modulus field, i.e., to the *EUI*s, separately taken.

Let us approximate the ith interval deviation $U_{i,j}^I$ by a rational function of the *EUI*s, so that Eq. (34) can be recast as:

$$U_j^I = U_{0,j} + \sum_{i=1}^{M} U_{i,j}^I = U_{0,j} + \sum_{i=1}^{M} \frac{\hat{e}_i^I}{A_{i,j} + B_{i,j}\hat{e}_i^I} \equiv U_j(\hat{e}_1^I, \hat{e}_2^I, \ldots, \hat{e}_M^I) \tag{35}$$

where $A_{i,j}$ and $B_{i,j}$ are $2M$ unknown coefficients. Following the philosophy of the *response surface method* [24], such coefficients can be estimated by selecting an appropriate *design of experiments*. A *saturated design* is herein applied which requires the evaluation of the exact implicit response U_j^I at $2M$ sampling points selected as follows: $\hat{e}_i^I = +1, \hat{e}_j^I = 0, i \neq j = 1, 2, \ldots, M; \hat{e}_i^I = -1, \hat{e}_j^I = 0, i \neq j = 1, 2, \ldots, M$. Thus, taking into account Eq. (35), the coefficients $A_{i,j}$ and $B_{i,j}$ can be obtained as solution of the following set of $2M$ linear algebraic equations:

$$U_j(0, \ldots, \hat{e}_i^I = +1, \ldots, 0) \equiv U_j^{(i)+} = U_{0,j} + \frac{1}{A_{i,j} + B_{i,j}}; \tag{36.1}$$

$$U_j(0, \ldots, \hat{e}_i^I = -1, \ldots, 0) \equiv U_j^{(i)-} = U_{0,j} + \frac{-1}{A_{i,j} - B_{i,j}}, \quad i = 1, 2, \ldots, M \tag{36.2}$$

where $U_{0,j}$, $U_j^{(i)+}$ and $U_j^{(i)-}$ are the jth components of the following vectors, respectively:

$$\mathbf{U}_0 = \mathbf{K}_0^{-1}\mathbf{F}; \tag{37.1}$$

$$\mathbf{U}^{(i)+} = (\mathbf{K}_0 + \mathbf{K}_i)^{-1}\mathbf{F}; \tag{37.2}$$

$$\mathbf{U}^{(i)-} = (\mathbf{K}_0 - \mathbf{K}_i)^{-1}\mathbf{F}, \quad i = 1, 2, \ldots, M. \tag{37.3}$$

In the previous equations, $\mathbf{K}_0$ is the nominal stiffness matrix (31), while $\mathbf{K}_i$ is the matrix defined by Eq. (32); $\mathbf{U}_0$ denotes the nominal displacement vector ($\hat{e}_i^I = 0, i = 1, 2, \ldots, M$); $\mathbf{U}^{(i)+}$ and $\mathbf{U}^{(i)-}$ are the deterministic displacement vectors obtained setting all the *EUI*s in the KL-like decomposition of the interval Young's modulus equal to zero except the ith which is set to $\hat{e}_i^I = +1$ and $\hat{e}_i^I = -1$, respectively. Notice that $2M + 1$ deterministic analyses are required.

By solving the set of equations (36.1,2), the following expressions of the unknown coefficients are derived:

$$A_{i,j} = \frac{U_j^{(i)-} - U_j^{(i)+}}{2\left(U_{0,j} - U_j^{(i)-}\right)\left(U_{0,j} - U_j^{(i)+}\right)}; \quad B_{i,j} = \frac{U_j^{(i)-} + U_j^{(i)+} - 2U_{0,j}}{2\left(U_{0,j} - U_j^{(i)-}\right)\left(U_{0,j} - U_j^{(i)+}\right)}, \tag{38.1,2}$$

$$j = 1, 2, \ldots, n; \; i = 1, 2, \ldots, M.$$

Once the coefficients $A_{i,j}$ and $B_{i,j}$ are known, Eq. (35) provides an approximate explicit relationship between the interval displacements and the *EUI*s.

In order to evaluate the bounds of the interval response, Eq. (35) is herein rewritten in the following *affine form*:

$$U_j^I = U_{0,j} + \sum_{i=1}^{M} U_{i,j}^I = U_{0,j} + \sum_{i=1}^{M} \left(a_{0i,j} + \Delta a_{i,j}\hat{e}_i^I\right) \tag{39}$$

where $a_{0i,j}$ and $\Delta a_{i,j}$ are the midpoint and deviation amplitude of the ith series term, i.e.:

$$a_{0i,j} = \frac{\bar{U}_{i,j} + \underline{U}_{i,j}}{2}; \qquad \Delta a_{i,j} = \frac{\bar{U}_{i,j} - \underline{U}_{i,j}}{2} > 0 \tag{40.1,2}$$

with

$$\underline{U}_{i,j} = \min\left\{\frac{-1}{A_{i,j} - B_{i,j}}, \frac{1}{A_{i,j} + B_{i,j}}\right\}; \qquad \bar{U}_{i,j} = \max\left\{\frac{-1}{A_{i,j} - B_{i,j}}, \frac{1}{A_{i,j} + B_{i,j}}\right\}. \tag{41.1,2}$$

Then, the LB and UB of the jth displacement component can be evaluated as follows:

$$\underline{U}_j = \text{mid}\left\{U_j^I\right\} - \sum_{i=1}^{M} \Delta a_{i,j}; \qquad \bar{U}_j = \text{mid}\left\{U_j^I\right\} + \sum_{i=1}^{M} \Delta a_{i,j} \tag{42.1,2}$$

where

$$\text{mid}\left\{U_j^I\right\} = U_{0,j} + \sum_{i=1}^{M} a_{0i,j} \tag{43}$$

is the midpoint value.

The bounds of the displacement field within the generic FE can be derived by applying the standard post-processing rules, i.e.:

$$\underline{w}^{(h)}(x) = \min_{\mathbf{d}^{(h)} \in \mathbf{d}^{(h)I}} \{\mathbf{N}^{(h)}(x)\mathbf{d}^{(h)}\} = \min_{\mathbf{U} \in \mathbf{U}^I} \{\mathbf{N}^{(h)}(x)\mathbf{L}^{(h)}\mathbf{U}\}; \tag{44.1}$$

$$\bar{w}^{(h)}(x) = \max_{\mathbf{d}^{(h)} \in \mathbf{d}^{(h)I}} \{\mathbf{N}^{(h)}(x)\mathbf{d}^{(h)}\} = \max_{\mathbf{U} \in \mathbf{U}^I} \{\mathbf{N}^{(h)}(x)\mathbf{L}^{(h)}\mathbf{U}\}. \tag{44.2}$$

Since $N_2^{(h)}(x) < 0$ and $N_j^{(h)}(x) > 0$ with $j \neq 2$, the previous relationships yield:

$$\underline{w}^{(h)}(x) = N_1^{(h)}(x)\underline{w}_1^{(h)} + N_2^{(h)}(x)\bar{\theta}_1^{(h)} + N_3^{(h)}(x)\underline{w}_2^{(h)} + N_4^{(h)}(x)\underline{\theta}_2^{(h)}; \tag{45.1}$$

$$\bar{w}^{(h)}(x) = N_1^{(h)}(x)\bar{w}_1^{(h)} + N_2^{(h)}(x)\underline{\theta}_1^{(h)} + N_3^{(h)}(x)\bar{w}_2^{(h)} + N_4^{(h)}(x)\bar{\theta}_2^{(h)} \tag{45.2}$$

where the bounds of the element nodal displacements, $\underline{w}_j^{(h)}$ and $\bar{w}_j^{(h)}$ $(j = 1, 2)$, and rotations, $\underline{\theta}_j^{(h)}$ and $\bar{\theta}_j^{(h)}$ $(j = 1, 2)$, are given by:

$$\underline{\mathbf{d}}^{(h)} = \left[\, \underline{w}_1^{(h)} \; \underline{\theta}_1^{(h)} \; \underline{w}_2^{(h)} \; \underline{\theta}_2^{(h)} \,\right]^{\mathrm{T}} = \mathbf{L}^{(h)}\underline{\mathbf{U}}; \tag{46.1}$$

$$\bar{\mathbf{d}}^{(h)} = \left[\, \bar{w}_1^{(h)} \; \bar{\theta}_1^{(h)} \; \bar{w}_2^{(h)} \; \bar{\theta}_2^{(h)} \,\right]^{\mathrm{T}} = \mathbf{L}^{(h)}\bar{\mathbf{U}} \tag{46.2}$$

with $\underline{\mathbf{U}}$ and $\bar{\mathbf{U}}$ collecting the LB and UB of the interval global displacements defined by Eq. (42.1,2).

5 Approximate explicit bounds of the interval bending moment

One of the main challenges to be faced in the context of interval finite element analysis is the evaluation of sharp bounds of the secondary variables which are more affected by the *dependency phenomenon* than the primary ones due to multiple occurrences of the interval variables describing the uncertain properties. In this section, attention is focused on the evaluation of the bounds of the interval bending moment $M^{(h)I}(x)$ at the generic abscissa x within the hth FE, defined as follows:

$$M^{(h)I}(x) = E^I(x)J_0(x)\chi^{(h)I}(x) = E^I(x)J_0(x)\mathbf{B}^{(h)}(x)\mathbf{d}^{(h)I}. \tag{47}$$

Taking into account Eq. (35) and replacing Eqs. (8) and (27) into Eq. (47), the following approximate explicit expression of the interval bending moment $M^{(h)I}(x)$ in terms of the *EUI*s is obtained:

$$M^{(h)}(x;\hat{e}_1^I,\hat{e}_2^I,\ldots,\hat{e}_M^I)=E_0J_0(x)\left[1+\sum_{i=1}^{M}\sqrt{\lambda_i}\ \psi_i(x)\hat{e}_i^I\right]\mathbf{B}^{(h)}(x)\mathbf{L}^{(h)}\mathbf{U}(\hat{e}_1^I,\hat{e}_2^I,\ldots,\hat{e}_M^I) \quad (48)$$

where $\mathbf{U}^I=\mathbf{U}(\hat{e}_1^I,\hat{e}_2^I,\ldots,\hat{e}_M^I)$ is the interval vector collecting the approximate interval global displacements defined in Eq. (35). By inspection of the previous relationship, it can be readily inferred that the interval bending moment $M^{(h)I}(x)$ depends on the *EUI*s both through the uncertain Young's modulus and the interval displacements. For this reason, the bounds of the interval bending moment could be highly overestimated unless a suitable approach, able to keep track of the dependencies between the *EUI*s, is applied. In view of the knowledge of the explicit relationship (48) and taking into account that at any abscissa x the output is a monotonic function of the *EUI*s, a sensitivity-based procedure can be conveniently adopted. To this aim, the *EUI*s are treated as variable parameters $\hat{e}_i\in\hat{e}_i^I=[-1,+1]$ collected into the vector $\hat{\mathbf{e}}$, and the sensitivities of the bending moment to these parameters are evaluated analytically by direct differentiation, i.e.:

$$s_{M^{(h)},i}(x)=\left.\frac{\partial M^{(h)}(x;\hat{e}_1,\hat{e}_2,\ldots,\hat{e}_M)}{\partial\hat{e}_i}\right|_{\hat{\mathbf{e}}=\mathbf{0}}. \quad (49)$$

Equation (49) provides information on the change of the bending moment at a prescribed abscissa x due to a change of the ith *EUI*, $\hat{e}_i^I$, within the range $[-1,+1]$. Specifically, $M^{(h)}(x;\hat{\boldsymbol{e}})$ is an increasing or decreasing function of $\hat{e}_i\in\hat{e}_i^I=[-1,+1]$ depending on whether $s_{M^{(h)},i}(x)>0$ or $s_{M^{(h)},i}(x)<0$, respectively. Then, based on the knowledge of the sensitivities $s_{M^{(h)},i}(x)$, $i=1,2,\ldots,M$, the combinations of the endpoints of the *EUI*s providing the LB and UB of the interval bending moment $M^{(h)I}(x)$, denoted by $\hat{e}_i^{(\mathrm{LB})}$ and $\hat{e}_i^{(\mathrm{UB})}$, respectively, can be determined as follows:

$$\text{if } s_{M^{(h)},i}(x)>0,\ \text{then } \hat{e}_i^{(\mathrm{UB})}=+1,\quad \hat{e}_i^{(\mathrm{LB})}=-1; \quad (50.1)$$

$$\text{if } s_{M^{(h)},i}(x)<0,\ \text{then } \hat{e}_i^{(\mathrm{UB})}=-1,\quad \hat{e}_i^{(\mathrm{LB})}=+1,\quad i=1,2,\ldots,M. \quad (50.2)$$

Then, the LB and UB of the interval bending moment $M^{(h)I}(x)$ can be evaluated in approximate explicit form by replacing the above defined combinations of the endpoints of the *EUI*s into Eq. (48), i.e.:

$$\underline{M}^{(h)}(x)=M^{(h)}(x;\hat{e}_1^{(\mathrm{LB})},\hat{e}_2^{(\mathrm{LB})},\ldots,\hat{e}_M^{(\mathrm{LB})});\ \bar{M}^{(h)}(x)=M^{(h)}(x;\hat{e}_1^{(\mathrm{UB})},\hat{e}_2^{(\mathrm{UB})},\ldots,\hat{e}_M^{(\mathrm{UB})}). \quad (51.1,2)$$

The previous relationships provide approximate explicit expressions of the bounds of the interval bending moment at the abscissa x within the hth FE.

6 Numerical applications

To validate the proposed IFE formulation, a cantilever beam and a fixed-simply supported beam with uncertain Young's modulus are selected as case studies. Both beams are characterized by the following geometrical and mechanical properties: length $L=5$ m; midpoint or nominal Young's modulus $E_0=3.85741\times10^8$ N/m^2; nominal moment of inertia $J_0=0.0054$ m^4. The uncertain Young's modulus is modeled as an *interval field* with exponential *spatial dependency function* (11). Different values of the parameters C_B and l_B are considered in order to analyze their effects on the bounds of the response. Decomposition (4) of the function $\Gamma_B(x,\xi)$ is performed retaining $M=20$ terms. For illustration purpose, Fig. 2 displays the LB and UB along with some samples of the interval Young's modulus over the domain of the beam for $C_B=0.05$ and two different values of the parameter l_B, say $l_B=0.5L$ and $l_B=5L$. Notice that as l_B increases, the samples of the uncertain material property become more regular so as to approach the condition of total spatial dependency where the interval field reduces to a single interval variable over the beam domain.

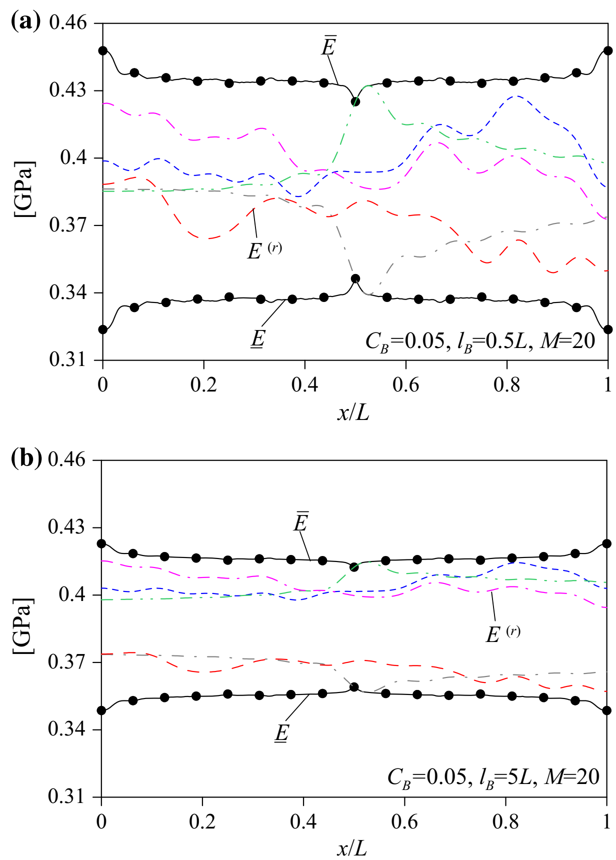

Fig. 2 LB and UB of the interval Young's modulus along with some samples $E^{(r)}$ for $C_B = 0.05$: **a** $l_B = 0.5L$ and **b** $l_B = 5L$

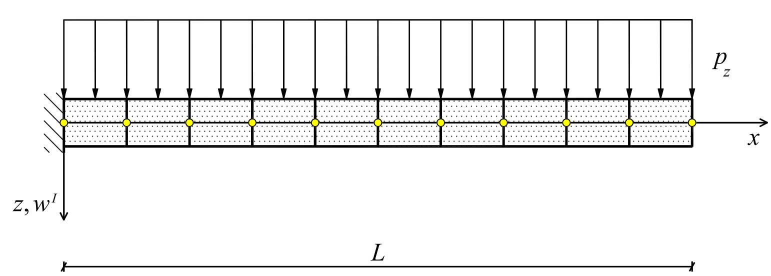

Fig. 3 Cantilever beam under uniformly distributed load with interval Young's modulus

6.1 Cantilever beam

The first example concerns a cantilever beam with interval Young's modulus subjected to a uniform transversal load per unit length $p_z = 10^3$ N/m (see Fig. 3). The beam is discretized into $N = 10$ IFEs of length $l_h = L/N = 0.5$ m.

For validation purpose, the proposed bounds of the interval displacement field are contrasted with those evaluated analytically by applying the procedure described in Ref. [27] for statically determinate beams with interval flexibility. Figure 4 shows a very good agreement between the LB and UB of the normalized deflection $w^I(x)E_0J_0/(p_zL^4)$ of the cantilever beam provided by the proposed IFE approach and the analytical bounds for $l_B = 0.5L$ and two different values of the parameter C_B, say $C_B = 0.05$ and $C_B = 0.1$.

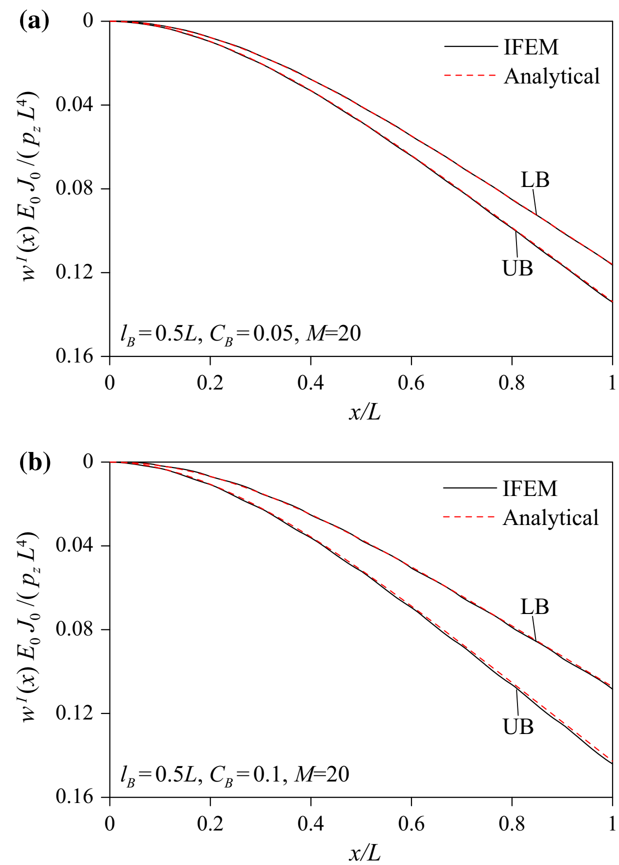

Fig. 4 LB and UB of the normalized deflection of the cantilever beam with interval Young's modulus: comparison between the analytical and IFEM solutions for $l_B = 0.5L$, **a** $C_B = 0.05$ and **b** $C_B = 0.1$

In order to investigate the influence of spatial dependency on the region of the interval response of the cantilever beam, the proposed bounds are compared with those obtained by applying the *vertex method* (VM) under the assumption of total spatial independency (TI) and total spatial dependency (TD). In the first case, Young's moduli of the FEs are modeled as independent interval variables $E_i^I = E_0(1 + \alpha_i^I)$, $i = 1, 2, \ldots, N$, where $\alpha_i^I = [-\Delta\alpha, \Delta\alpha]$ are symmetric interval variables and $\Delta\alpha$ is consistently set equal to C_B. In the second case, the uncertain Young's modulus is modeled as an interval variable over the whole domain, i.e., $E^I = E_0(1 + C_B\hat{e}^I)$. It is recalled that, for a problem involving N interval variables, the VM requires to perform 2^N deterministic analyses, as many as are the possible combinations of the endpoints of uncertainties, and then to evaluate the LB and UB of the response as the minimum and maximum among the solutions so obtained. Figure 5 shows that, for $l_B = 0.5L$ and two different values of C_B, the region predicted by using the proposed interval Euler–Bernoulli FE, incorporating the interval field representation of the uncertain Young's modulus, is larger than that pertaining to the limit cases of TI and TD uncertainty. In particular, the bounds obtained under the assumptions of TI and TD interval Young's modulus are the same for the selected example since they are achieved when all the interval variables are set simultaneously at their LB or UB. Of course, this is not generally the case.

Once the accuracy and consistency of the proposed IFE formulation have been assessed, attention is focused on the convergence rate of the solution (35) with the number M of terms of the KL-like decomposition of the interval Young's modulus as well as on the influence of the spatial dependency on the response. Figure 6 displays the LB and UB of the interval tip displacement versus the number M of series terms for $C_B = 0.05$ and different values of the parameter l_B governing the spatial dependency. It is observed that, as the parameter l_B increases, the series converges more quickly so that a smaller number of terms is required. Furthermore, it can be seen that, when larger values of l_B are considered, the UB and LB of the tip displacement decrease and increase, respectively, and in the limit, as $l_B \to \infty$, the bounds pertaining to the case of a totally spatially dependent

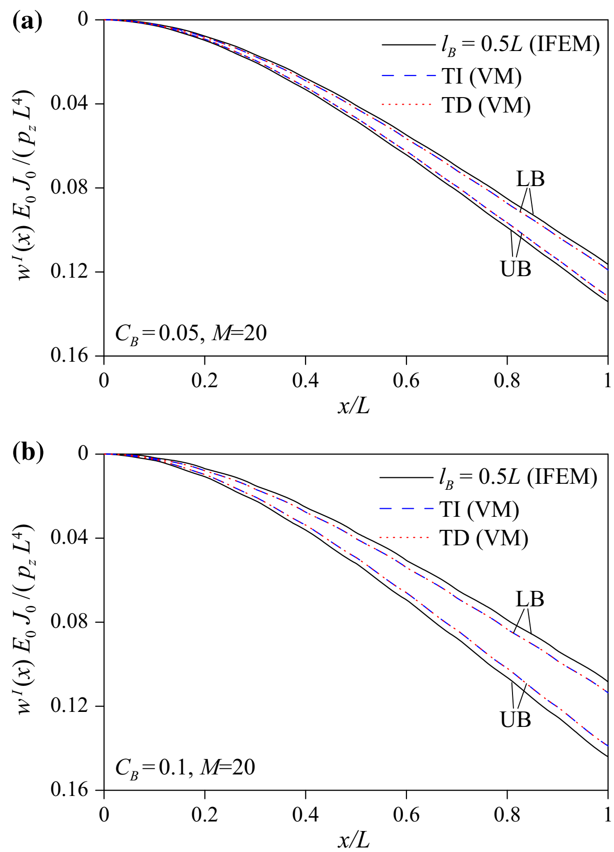

Fig. 5 Comparison between the bounds of the normalized deflection of the cantilever beam obtained by applying the proposed IFEM with $l_B = 0.5L$ and by the VM under the assumption of total spatial independency (TI) and total spatial dependency (TD) of the interval Young's modulus for **a** $C_B = 0.05$ and **b** $C_B = 0.1$

Young's modulus are approached. In order to further scrutinize the influence of the spatial dependency on the response, the so-called *coefficient of interval uncertainty* (c.i.u.) of the tip displacement is evaluated. Such a coefficient, defined as c.i.u.$[w^I(L)] = \Delta w(L)/\left|\text{mid}\{w^I(L)\}\right|$, provides a measure of the dispersion of the response around the midpoint value. Figure 7 shows the c.i.u. of the tip displacement versus the number M of series terms for $C_B = 0.05$ and different values of the parameter l_B with $0.5L \leq l_B \leq 10L$. Obviously, also in this case, the convergence rate increases with l_B. Furthermore, as the parameter l_B decreases within the considered range, a larger dispersion of the response around the midpoint value is detected. Conversely, as the parameter l_B increases the c.i.u. tends to the value $C_B = 0.05$ pertaining to the case of a totally spatially dependent Young's modulus [21,22,27].

6.2 Fixed-simply supported beam

As second example, let us consider a fixed-simply supported beam with uncertain Young's modulus subjected to a uniform transversal load per unit length $p_z = 2 \times 10^4$ N/m and a concentrated moment $M = 10^5$N m at $x = L$ (see Fig. 8). The beam is discretized into $N = 10$ Euler–Bernoulli IFEs of length $l_h = L/N = 0.5$ m.

The accuracy of the proposed bounds of the interval displacement field is assessed by comparison with those obtained by applying a recently proposed FD scheme based on the use of the *IRSE* [21] and with the exact bounds provided by the VM. The latter requires 2^M deterministic FE analyses of the beam, as many as are the possible combinations of the endpoints of the *EUI*s appearing in the definition of the interval Young's modulus (8) and consequently in the approximate explicit expression (35) of the interval global displacements. Figure 9 shows that the proposed bounds of the normalized deflection $w^I(x)E_0J_0/(p_zL^4)$ are in very good

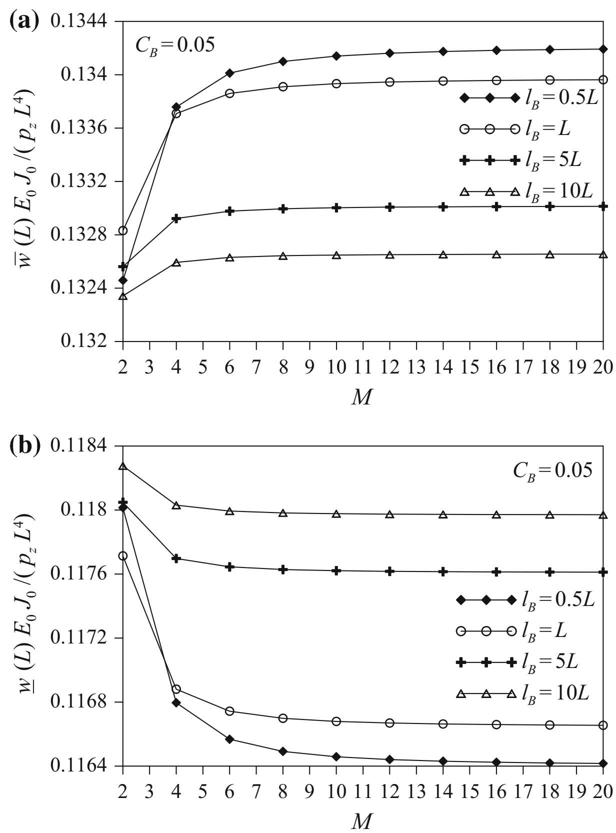

Fig. 6 **a** UB and **b** LB of the normalized tip deflection of the cantilever beam with interval Young's modulus versus the number M of terms of the KL-like decomposition for different values of the parameter l_B ($C_B = 0.05$)

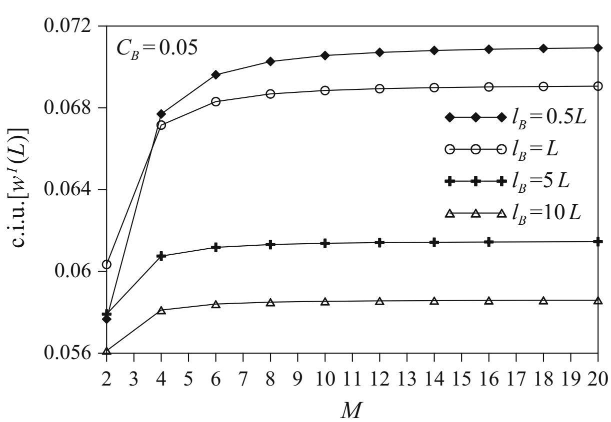

Fig. 7 *Coefficient of interval uncertainty* of the normalized tip deflection of the cantilever beam with interval Young's modulus versus the number M of terms of the KL-like decomposition for different values of the parameter l_B ($C_B = 0.05$)

agreement with both the exact ones and those predicted by the FD scheme for $l_B = 0.5L$ and two different values of the parameter C_B, say $C_B = 0.05$ and $C_B = 0.1$. Furthermore, it is observed that IFE and FD solutions exhibit the same degree of accuracy as the uncertainty level increases (see Fig. 9b). In Fig. 10, the region of the interval displacement along the beam provided by the proposed IFE formulation is compared with that obtained under the assumptions of TI and TD interval Young's modulus. As in the previous example, it is observed that the interval field model, with $l_B = 0.5L$ and two different values of C_B, yields a wider region

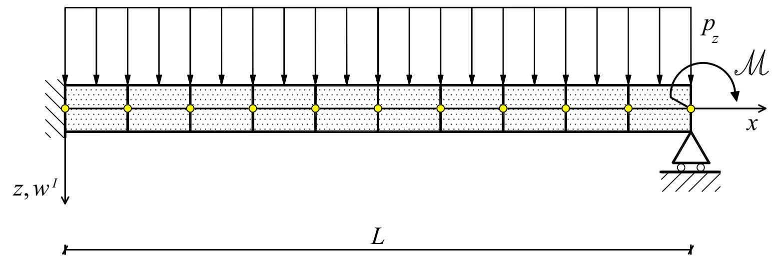

Fig. 8 Fixed-simply supported beam under uniformly distributed load and concentrated moment at $x = L$ with interval Young's modulus

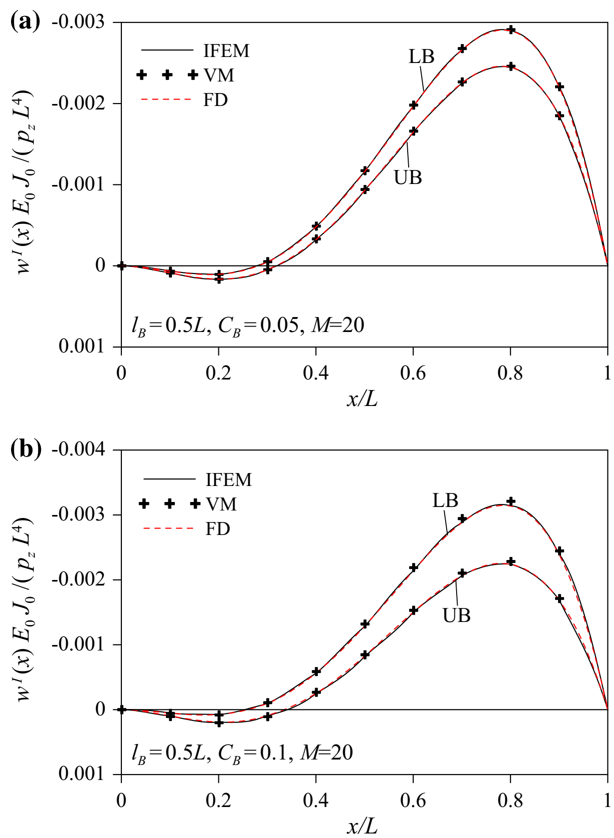

Fig. 9 LB and UB of the normalized deflection of the fixed-simply supported beam with interval Young's modulus: comparison between the solutions provided by the proposed IFEM, the VM and an FD scheme for $l_B = 0.5L$, **a** $C_B = 0.05$ and **b** $C_B = 0.1$

of the response, thus demonstrating the key role played by the spatial dependency of the uncertain material property.

Table 1 lists the LB and UB of the interval bending moment, $M_1^I = M^I(x)\big|_{x=0}$, at the abscissa $x = 0$ of the beam with the interval Young's modulus evaluated by applying the sensitivity-based procedure proposed in Sect. 5 and the VM, for $l_B = 0.5L$ and two different values of the parameter C_B, say $C_B = 0.05$ and $C_B = 0.1$. The associated absolute percentage errors are also reported. Notice that the proposed bounds are in very good agreement with the exact ones, even when the uncertainty level increases.

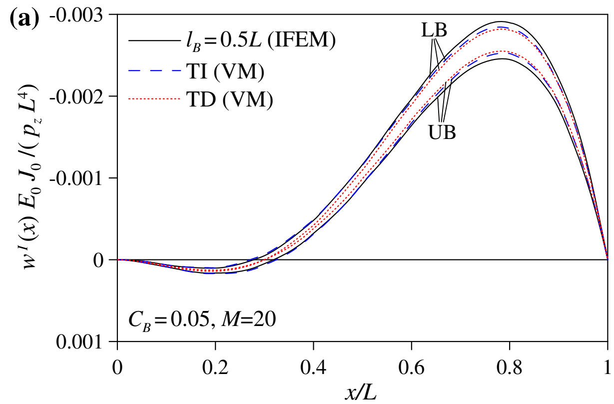

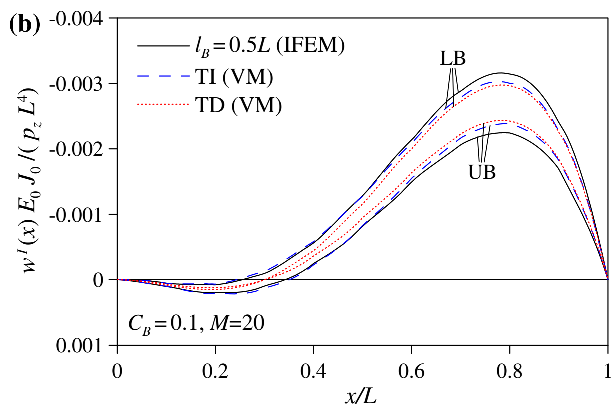

Fig. 10 Comparison between the bounds of the normalized deflection of the fixed-simply supported beam obtained by applying the proposed IFEM with $l_B = 0.5L$ and by the VM under the assumption of total spatial independency (TI) and total spatial dependency (TD) of the interval Young's modulus for **a** $C_B = 0.05$ and **b** $C_B = 0.1$

Table 1 LB and UB of the interval bending moment M_1^I evaluated at $x = 0$ by applying the proposed IFEM and the VM, along with the associated absolute percentage errors

M_1^I (Nm)	LB			UB		
	IFEM	VM	ε_{M_1} (%)	IFEM	VM	$\varepsilon_{\bar{M}_1}$ (%)
$C_B = 0.05$	−12957.268	−12917.998	0.303	−11284.003	−11250.384	0.298
$C_B = 0.1$	−13919.814	−13750.363	1.232	−10546.701	−10385.688	1.550

7 Conclusions

An interval finite element formulation incorporating spatially variable uncertainty into the traditional Euler–Bernoulli beam element has been developed. The key idea is to integrate the concept of an interval field into the standard finite element formulation. To this aim, a recently proposed interval field model based on the so-called *improved interval analysis via extra unitary interval* has been adopted to describe the uncertain property. Then, the propagation of the interval field has been efficiently performed assuming an appropriate *response surface* to approximate the interval output.

The main features of the proposed approach may be summarized as follows: (i) the spatial dependency of the interval uncertainty is accounted for, thus allowing to overcome the inherent limitation of traditional interval finite element methods which assign independent interval variables to the finite elements; (ii) the number of deterministic analyses required to estimate the bounds of the interval response is drastically reduced compared to combinatorial procedures; (iii) the main steps of the deterministic finite element method are kept unaltered, thus allowing the integration into commercial software; (iv) very accurate estimates of the bounds of both primary and secondary variables are obtained.

Future research will focus on the extension of the proposed interval finite element formulation to the analysis of two-dimensional problems involving spatially variable interval uncertainties.

References

1. Schmelzer, B., Oberguggenberger, M., Adam, C.: Efficiency of tuned mass dampers with uncertain parameters under stochastic excitation. Proc. Inst. Mech. Eng. O: J. Risk Reliab. **224**(4), 297–308 (2010)
2. Adam, C., Heuer, R., Ziegler, F.: Reliable dynamic analysis of an uncertain compound bridge under traffic loads. Acta Mech. **223**, 1567–1581 (2012)
3. Stefanou, G.: The stochastic finite element method: past, present and future. Comput. Methods Appl. Mech. Eng. **198**, 1031–1051 (2009)
4. Moore, R.E., Kearfott, R.B., Cloud, M.J.: Introduction to Interval Analysis. SIAM, Philadelphia (2009)
5. Ben-Haim, Y., Elishakoff, I.: Convex Models of Uncertainty in Applied Mechanics. Elsevier, Amsterdam (1990)
6. Qiu, Z., Elishakoff, I.: Antioptimization of structures with large uncertain-but-non-random parameters via interval analysis. Comput. Methods Appl. Mech. Eng. **152**, 361–372 (1998)
7. Köylüoğlu, H.U., Elishakoff, I.: A comparison of stochastic and interval finite elements applied to shear frames with uncertain stiffness properties. Comput. Struct. **67**, 91–98 (1998)
8. Muhanna, R.L., Mullen, R.L.: Uncertainty in mechanics problems-interval-based approach. J. Eng. Mech. ASCE **127**, 557–566 (2001)
9. Degrauwe, D., Lombaert, G., De Roeck, G.: Improving interval analysis in finite element calculations by means of affine arithmetic. Comput. Struct. **88**, 247–254 (2010)
10. Rama Rao, M.V., Mullen, R.L., Muhanna, R.L.: A new interval finite element formulation with the same accuracy in primary and derived variables. Int. J. Reliab. Saf. **5**, 336–357 (2011)
11. Sofi, A., Romeo, E.: A novel interval finite element method based on the improved interval analysis. Comput. Methods Appl. Mech. Eng. **311**, 671–697 (2016)
12. Moens, D., Vandepitte, D.: A survey of non-probabilistic uncertainty treatment in finite element analysis. Comput. Methods Appl. Mech. Eng. **194**, 1527–1555 (2005)
13. Moens, D., Hanss, M.: Non-probabilistic finite element analysis for parametric uncertainty treatment in applied mechanics: recent advances. Finite Elem. Anal. Des. **47**, 4–16 (2011)
14. Muscolino, G., Sofi, A.: Stochastic analysis of structures with uncertain-but-bounded parameters via improved interval analysis. Probab. Eng. Mech. **28**, 152–163 (2012)
15. Moens, D., De Munck, M., Desmet, W., Vandepitte, D.: Numerical dynamic analysis of uncertain mechanical structures based on interval fields. In: Belyaev, A.K., Langley, R.S. (eds.) IUTAM Symposium on the Vibration Analysis of Structures with Uncertainties, pp. 71–83. Springer, Dordrecht (2011)
16. Verhaeghe, W., Desmet, W., Vandepitte, D., Moens, D.: Interval fields to represent uncertainty on the output side of a static FE analysis. Comput. Methods Appl. Mech. Eng. **260**, 50–62 (2013)
17. Vanmarcke, E.: Random Fields: Analysis and Synthesis. Revised and Expanded New Edition. World Scientific, Singapore (2010)
18. Imholz, M., Faes, M., Cerneels, J., Vandepitte, D., Moens, D.: On the comparison of two novel interval field formulations for the representation of spatial uncertainty. In: Freitag, S., Muhanna, R.L., Mullen, R.L. (eds.) Proceedings of the 7th International Workshop on Reliable Engineering Computing (REC2016), June 15–17, 2016. Ruhr University Bochum, Germany, pp. 367–378 (2016)
19. Faes, M., Cerneels, J., Vandepitte, D., Moens, D.: Identification and quantification of multivariate interval uncertainty in finite element models. Comput. Methods Appl. Mech. Eng. **315**, 896–920 (2017)
20. Muscolino, G., Sofi, A., Zingales, M.: One-dimensional heterogeneous solids with uncertain elastic modulus in presence of long-range interactions: interval versus stochastic analysis. Comput. Struct. **122**, 217–229 (2013)
21. Sofi, A., Muscolino, G.: Static analysis of Euler–Bernoulli beams with interval Young's modulus. Comput. Struct. **156**, 72–82 (2015)
22. Sofi, A., Muscolino, G., Elishakoff, I.: Static response bounds of Timoshenko beams with spatially varying interval uncertainties. Acta Mech. **226**, 3737–3748 (2015)
23. Wu, D., Gao, W.: Hybrid uncertain static analysis with random and interval fields. Comput. Methods Appl. Mech. Eng. **315**, 222–246 (2017)
24. Bucher, C.: Computational Analysis of Randomness in Structural Mechanics. Taylor & Francis, London (2009)
25. Dong, W., Shah, H.: Vertex method for computing functions of fuzzy variables. Fuzzy Sets Syst. **24**, 65–78 (1987)
26. Ghanem, R.G., Spanos, P.D.: Stochastic Finite Elements: A Spectral Approach. Springer, New York (1991)
27. Sofi, A.: Structural response variability under spatially dependent uncertainty: stochastic versus interval model. Probab. Eng. Mech. **42**, 78–86 (2015)